Wind- and buoyancy-forced upper ocean circulation in two-strait marginal seas with application to the Japan/East Sea

Michael A. Spall

Department of Physical Oceanography, Woods Hole Oceanographic Institution, Woods Hole, Massachusetts, USA

Received 3 May 2001; revised 20 September 2001; accepted 27 September 2001; published 11 January 2002.

[1] The wind- and buoyancy-forced upper ocean circulation in a marginal sea connected to the open ocean through two straits is investigated using idealized numerical and analytical models. The study is motivated by the Japan/East Sea (JES) and other marginal seas found along the western North Pacific. It is shown that for anticyclonic wind stress curl and atmospheric cooling in the marginal sea, the inflow transport branches into eastern and western boundary currents, in qualitative agreement with observed branching of the Tsushima Current in the southern JES. The eastern boundary current arises because wind forcing in the open ocean, and a circulation integral around the island that separates the marginal sea from the open ocean, maintains the temperature on the island to be warmer than that found in the interior of the marginal sea. Buoyancy forcing in the marginal sea plays a key role in maintaining the eastern boundary current. The dynamics that control the water mass transformation and downwelling are described and related to the model parameters. The largest heat loss to the atmosphere is found in the eastern boundary current. The exchange rates with the open ocean, downwelling within the marginal sea, and current structure within the marginal sea predicted by a linear analytic theory compare closely with results from a shallow water numerical model. *INDEX TERMS:* 4243 Oceanography: General: Marginal and semienclosed seas, 4516 Oceanography: Physical: Eastern boundary currents, 4532 Oceanography: Physical: General circulation, 4572 Oceanography: Physical: Upper ocean processes; *KEYWORDS:* Eastern boundary currents, marginal seas, straits, Japan Sea

1. Introduction

[2] The Japan/East Sea (JES) is a semienclosed marginal sea bounded by the Asian continent to the west and the Japanese islands to the east. The Tsushima Current flows into the JES through the Tsushima Strait from the East China Sea to the south (Figure 1). This water flows out of the JES into the Pacific Ocean through the Tsugaru Strait and into the Sea of Okhotsk to the north through the Soya and Tartar Straits. There is a net heat loss to the atmosphere in the JES [*Hirose et al.*, 1996], so that the outflowing water is cooler than the inflowing water. One of the dominant flow features within the JES is the splitting of the Tsushima Current into eastern and western boundary current branches just after it enters the JES (Figure 1). The western branch is called the East Korean Warm Current. Although still a point of some debate, there are generally thought to be two eastern branches [*Kawabe*, 1982a]. The Nearshore Branch, or First Branch, follows the 100 m isobath, and the more time-dependent Second Branch is found offshore of the Nearshore Branch [*Hase et al.*, 1999]. A recent review of the circulation in the JES and adjacent Sea of Okhotsk is given by *Preller and Hogan* [1998].

[3] Numerous theories have been proposed for the branching of the Tsushima Current. Most are adiabatic in nature and rely on some form of time-dependent wind forcing, potential vorticity conservation, or frictional control. *Yoon* [1982a] suggested that the Nearshore Branch arises as a result of conservation of potential vorticity and stretching induced by the sloping bottom as the Tsushima Current enters the JES. This stretching results in a trapping of the transport over the shallow topography as it turns toward the east. *Kawabe* [1982b] extended this idea to consider a baroclinic current and found that the Nearshore Branch could be supported by shallow topography and that an offshore current could be formed with time-dependent inflow transport and a deep sloping bottom. *Sekine* [1986] also found that time dependence in the wind stress could result in an eastern branch in the summer, consistent with the observations of *Kawabe* [1982a].

[4] Two recent ideas for the branching of the Tsushima Current rely on processes within the Tsushima Strait. *Cho and Kim* [2000] proposed that a branching of the Tsushima Current may result within the Tsushima Strait as a result of seasonal variations in the extent to which dense waters penetrate into the strait from the JES. *Ou* [2001] has developed a simple model in which hydraulic control and friction acting on a flow through a channel produce a two-jet structure reminiscent of the branching of the Tsushima Current.

[5] There have also been several studies that suggest that buoyancy forcing may be important for the branching of the inflow. *Yoon and Suginohara* [1977] recognized that warm water flowing into a cold basin would result in a geostrophically balanced eastern boundary current. However, long integrations of their adiabatic model resulted in westward propagation of the inflowing warm waters and an eventual warming of the marginal sea and a shift of the eastern boundary current all the way to the western boundary. *Yoon* [1982b] also considered a warm inflow and found that an eastern branch was supported in summer and fall but not in winter or spring. Yoon suggested that the seasonal disappearance of the eastern branch may be related to errors in the salinity near the eastern boundary.

[6] Analysis of hydrographic and direct current measurements by *Hase et al.* [1999] suggests that the Nearshore Branch is topographically controlled and remains trapped near the 100 m isobath all along the west coast of Japan. However, the location of the Second Branch is much more time dependent and appears to be

0148-0227/2001JC000966

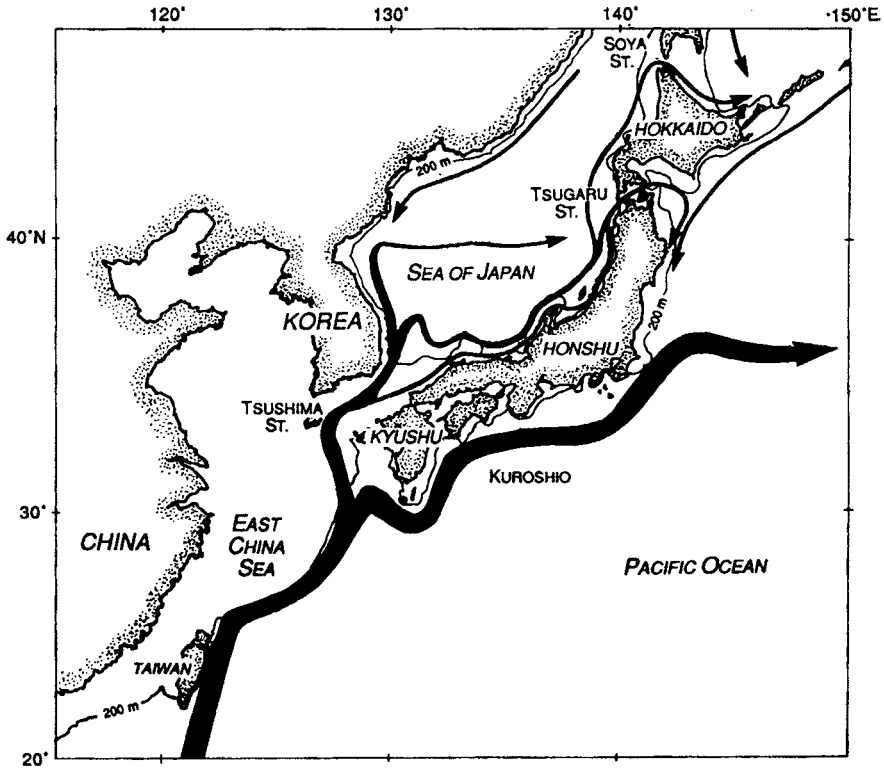

Figure 1. Schematic of the circulation in the Sea of Japan and western Pacific Ocean [from *Nof*, 1993].

correlated with the shelf break only to the west of the Noto Peninsula, just downstream of the Tsushima Strait. To the north and east of Noto Peninsula, over most of its path through the JES, the Second Branch is found well offshore of the shelf break, indicating that topographic control is minimal.

[7] *Hogan and Hurlburt* [2000] were able to produce realistic upper ocean currents, including a branching of the Tsushima Current, in a nonlinear, high-resolution, wind- and buoyancy-forced numerical model of the JES. They find, however, that even with time dependent wind forcing and bottom topography, the eastern branch is only produced when buoyancy forcing is included in the model. A similar branching is found when the bottom is flat. These results suggest that buoyancy forcing is playing the key role in the branching of the Tsushima Current in their model.

[8] The mass and property exchanges between marginal seas and the open ocean when they are connected by a single strait is predominantly baroclinic, and hydraulic controls often limit the transport through the strait. The fundamentally different nature of the exchange when a second strait is introduced can be anticipated by application of a circulation integral around the island formed by the two straits. *Godfrey* [1989] derived a simple and powerful integral constraint to estimate the net mass flux between the Pacific and Indian Oceans (the island being Australia), which is often referred to as the island rule. The introduction of a second strait permits a barotropic circulation to pass through the marginal sea because the pressure on the island can be much different than it is on the basin perimeter. *Minato and Kimura* [1980] recognized the importance of having two straits connecting the JES to the Pacific Ocean and applied a similar circulation integral to estimate the wind-driven exchange. *Nof* [2000] compared numerical model predictions of the transport through marginal seas with Godfrey's island rule, *Nof*'s [1993] beta control, and the circulation integral of *Minato and Kimura* [1980] as a function of the latitude of the marginal sea. It was concluded that the relatively small circulation through the Sea of Japan results from its location at midlatitudes. *Pedlosky et al.* [1997] extended Godfrey's island rule to consider a variety of island configurations and tested the linear theory with nonlinear numerical model and laboratory experiments over a wide range of parameters. It was found that the linear estimate was reasonably accurate even when nonlinearities were very large and straits were relatively narrow. These previous studies have considered only the wind-driven barotropic transport and have neglected dissipation on the western side of the island and mass sources/sinks to the east of the island and in the marginal sea.

[9] In two recent studies, *Spall* [2000, also on the baroclinic structure of the Indonesian throughflow, submitted to *Journal of Physical Oceanography*, 2001, hereinafter referred to as Spall, submitted manuscript 2001] showed that buoyancy forcing can also force strong baroclinic circulations around islands in two distinct ways. Diapycnal mixing in the open ocean to the east of an island introduces a mass source/sink in the isopycnal layers. The along isopycnal mass flux at a latitude north of the mixing will then differ from the mass flux to the south of the mixing. Provided that the mixing is not near a boundary, the only way that both mass and vorticity budgets can be satisfied is through the development of a strong horizontal recirculation gyre. For the case of mixing to the east of an island, some of this recirculation gyre will, in general, extend around the island and into the marginal sea. Diapycnal mixing can also force an exchange between basins if the mixing is concentrated along the western side of the island because dissipation becomes important there, although dissipation can generally be neglected on the west coast of the island for purely wind-driven calculations [*Godfrey*, 1989; *Wajsowicz*, 1993; *Pedlosky et al.*, 1997].

[10] The main objective of the present study is to understand how the exchange in the upper ocean between a marginal sea with more than one strait and the open ocean depends on the surface heat flux in the marginal sea. (It should be clear that similar dynamics would apply to adjacent abyssal basins separated by mid-ocean ridges and forced by diapycnal mixing.) This requires an understanding of what controls the transports into and out of the

marginal sea, which in turn depends on how the currents navigate through the marginal sea. If the marginal sea is subject to cooling and anticyclonic wind stress curl, as is the southern JES, then the inflow can branch into eastern and western boundary currents. A major difference between this study and most previous models of the JES is that the exchanges through the straits are not imposed, but rather allowed to adjust to the model physics and forcing both within the marginal sea and in the open ocean.

[11] Examples of the branching in a marginal sea produced in a numerical model with wind and buoyancy forcing are shown in section 2. The boundary layer structure and its dependence on the environmental parameters are explored through the development of a simple analytic model in section 3. Comparisons of the exchange rates and downwelling between model and theory are presented and discussed in section 4, and a final summary is given in section 5.

2. Influences of Buoyancy Fluxes in the Marginal Sea

[12] The general response of a marginal sea subject to a net surface heat flux and connected to the open ocean through two straits is explored using a shallow water numerical model. The model integrates the nondimensional shallow water momentum and continuity equations subject to wind and buoyancy forcing. Details of the equations and numerical solution procedure can be found in Appendix A.

[13] The importance of nonlinearity, dissipation, and buoyancy forcing can be characterized by their relevant length scales. The Munk layer thickness $\delta_M = (A_h/\beta^*)^{1/3}$, where A_h is a lateral eddy viscosity coefficient and β^* is the meridional gradient in planetary vorticity, is a measure of the importance of lateral viscosity. The inertial boundary layer thickness $\delta_I = (U/\beta^*)^{1/2}$, where U is a typical velocity in the basin interior, is a measure of the strength of the nonlinear terms. The thermal length scale $\delta_T = \beta^* L_d^2 t_T$, where t_T is a thermal damping timescale and L_d is the internal deformation radius, is the distance a baroclinic Rossby wave can propagate before it is damped by buoyancy forcing. A large value of δ_T indicates that buoyancy forcing is weak.

[14] The model is run by specifying the boundary layer widths δ_M, δ_I, δ_T, the Burger number $B = (L_d/L)^2$, the relative variation of the Coriolis parameter $\beta = \beta^* L/f_0$, and the domain size L_x and L_y. The Coriolis parameter is assumed to vary linearly with latitude as $f = f_0 + \beta^* y$. The nondimensional numbers required to integrate the shallow water equations (see Appendix A) are the Rossby number $R = \beta\delta_I^2$, an Ekman number $E = \beta\delta_M^3$, and a thermal restoring coefficient $\gamma = B/\delta_I^2\delta_T$.

[15] Because the region of interest is the southern JES (south of the subpolar front near 40°N, Figure 1), only cases of anticyclonic wind stress curl will be considered [*Na et al.*, 1992]. Cyclonic wind stress curl calculations have been carried out, and many of the dynamical processes are easily generalized to these cases. The nondimensional wind stress is taken to be zonal only with meridional distribution

$$\tau = -\frac{1}{\pi}\cos\left(\pi(y - y_0)/L_y\right), \qquad (1)$$

where y_0 is the southern latitude of the domain.

[16] The runs discussed here are all in the linear regime and the boundary layer widths are small compared to the basin dimension; $\delta_M/L = 0.01$ and $\delta_I/L = 0.001$. The strength of the thermal damping δ_T/L will be varied between 0.01 and 0.08. The Burger number $B = 0.01$, but the results are not overly sensitive to this choice. The nondimensional variation of the Coriolis parameter is typical of midlatitude basins, $\beta = 0.4$.

[17] The standard case considered is a square basin of dimension $L_x = L_y = 1$ which contains an island extending from $y_s = 0.133$ to $y_n = 0.866$ (giving an island dimension $L_i = y_n - y_s = 0.73$) and from $x_w = 0.47$ to $x_e = 0.53$. To the west of $x = x_e$ the basin perimeter also extends southward from the northern boundary to $y = 0.9$ and northward from the southern boundary to $y = 0.1$ (see Figure 2). The basin to the east of this long, narrow island is referred to as the open ocean, and the basin to the west is the marginal sea. The grid resolution is 151 by 151.

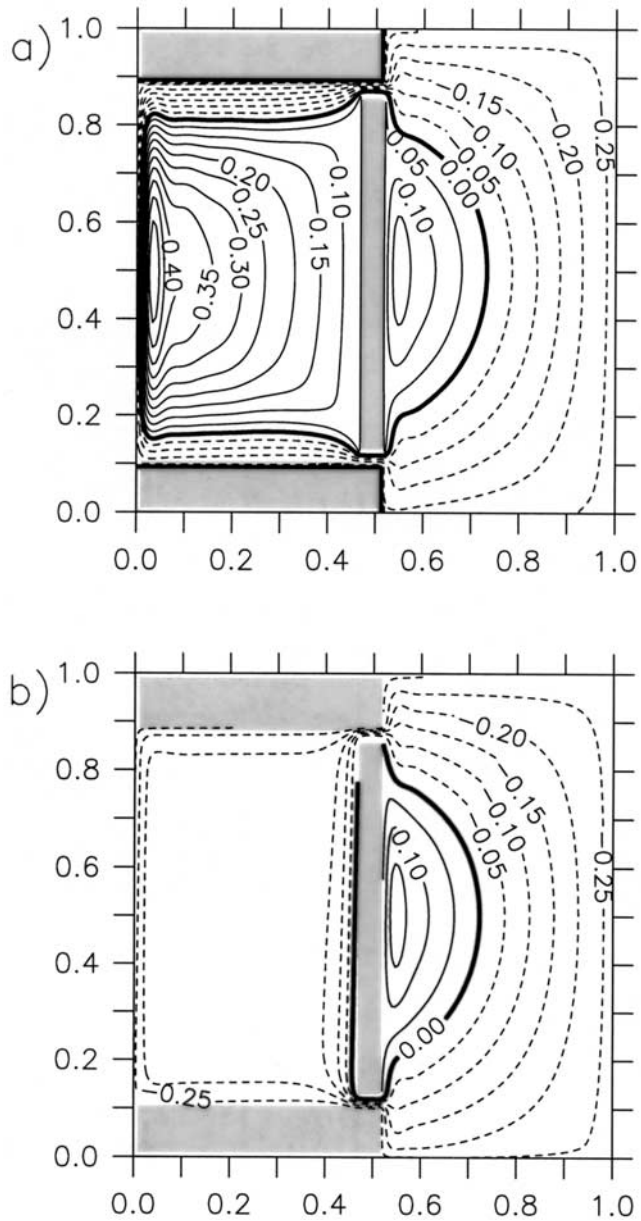

Figure 2. Upper layer thickness from a shallow water numerical model for (a) wind forcing only and (b) wind and buoyancy forcing with $\delta_T = 0.02$ and strong damping east of the island ($\alpha = 15$).

[18] Variations in layer thickness in this simple model may also be thought of as lateral variations in upper ocean temperature such that a thin layer corresponds to cold water and a thick layer corresponds to warm water. The flow is nearly in geostrophic balance, so that the general flow direction is along lines of constant h with warm (thick) water to the right in the Northern Hemisphere.

2.1. Wind Forcing Only

[19] The anticyclonic wind stress curl forces subtropical gyres in both the open ocean and the marginal sea, as indicated in Figure 2. The circulation to the east of the island contains a large-scale

anticyclonic recirculation with stagnation points at two latitudes on the eastern side of the island (y = 0.27, 0.73). This recirculation is required to balance the circulation integral around the island, as discussed by *Pedlosky et al.* [1997]. For this purely wind forced case, the dissipation along the western, northern, and southern sides of the island is negligible, so that the net dissipation along the eastern side of the island must vanish. This is achieved by having a reversal in the meridional velocity, thus giving rise to the stagnation points and the closed recirculation along the eastern side of the island.

[20] There is an anticyclonic circulation through the marginal sea of (nondimensional) strength $T = 0.36$, compared to a maximum southward Sverdrup flow in the eastern basin of 0.47. This throughflow compares closely with the estimate based on Godfrey's Island Rule, which in the present nondimensional formulation is simply $T = [\tau(y_n) - \tau(y_s)](1 - x_w)/L_i = 0.38$. The circulation in the interior of the marginal sea is everywhere toward the south. The inflow from the open ocean flows along the southern boundary until it encounters the western boundary, where it then flows all the way to the northern boundary, turns to the east and finally exits the marginal sea through the northern strait. This general sense of the upper ocean circulation is similar to that found by *Hogan and Hurlburt* [2000] using realistic wind and inflow/outflow forcing in a high resolution primitive equation model both with and without bottom topography.

2.2. Wind and Buoyancy Forcing

[21] The effects of buoyancy forcing in the marginal sea are now considered. Density anomalies that are generated within the marginal sea enter the open ocean through the northern and southern straits as Kelvin waves. These waves propagate cyclonically around the basin and allow the thickness of the upper layer to adjust such that circulation integrals around the basin and island are satisfied. With a continental slope, this same role would be filled by coastally trapped topographic waves. The larger size of the real open ocean compared to the marginal sea is parameterized here by strongly restoring the upper layer thickness toward that of the purely wind-driven solution (Figure 2) to the east of $x = 0.6$. Strong in this context means that Kelvin waves are damped before they can circumnavigate the open ocean domain. For these cases, the thickness of the upper layer at the southern boundary of the southern strait (and thus the strength of the inflow) will be modified by the Kelvin waves, but the thickness of the upper layer on the eastern and northern boundaries of the open ocean will remain unchanged from the purely wind-driven case.

[22] It is useful to treat the thermal forcing in the region just to the east of the island, between $x = 0.53$ and $x = 0.6$, in two limits. For the cases where the damping is sufficiently strong that a Kelvin wave cannot circumnavigate the island, the thickness at the southern end of the island will be uninfluenced by the heat flux in the marginal sea and identical to that found in the purely wind-driven case. On the other hand, if damping is weak, Kelvin waves may propagate all the way around the island to alter the upper layer thickness at $y = y_s$, and thus also influence the transport into the marginal sea. The thickness of the outflow at the northern tip of the island will be altered by buoyancy forcing in the marginal sea; however, the strength of this outflow does depend on the damping of coastal waves along the eastern coast of the island. The importance of buoyancy forcing east of the island is indicated by the ratio of the meridional length scale of the island to the distance a Kelvin wave can propagate over the thermal damping timescale, $\alpha = L_I \beta B^{1/2}/\delta_T$. For $\alpha \ll 1$, a Kelvin wave can propagate around the island before it is damped, and so in this regime the island is referred to as small. For $\alpha \gg 1$, the island is referred to as large because the temperature at the southern tip of the island is unchanged by buoyancy forcing in the marginal sea.

[23] For simplicity, the upper layer thickness in the marginal sea ($0 < x < x_w$) is restored toward a uniform thickness, $h^* = H^*$ (see equation (A2)). Note that a uniform atmospheric temperature does not imply a uniform heat flux into/out of the ocean. The heat flux is proportional to the air-sea temperature (or thickness) difference. The spatial variability of the net surface heat flux is determined by the spatial variability in the upper ocean temperature and takes on the spatial scales of the ocean currents. This may be thought of as a crude parameterization of the latent and sensible heat flux components. To the east of the marginal sea ($x > x_w$), the upper layer thickness is restored toward the purely wind-driven solution shown in Figure 2a, $h^* = h_w(x, y)$.

[24] The focus here is on cooling within the marginal sea because in the annual mean the net heat flux in the southern JES is from the ocean to the atmosphere [*Hirose et al.*, 1996]. There are two important points related to the neglect of the seasonal cycle. The first is that it is the spatial variability of the surface heat flux that dominates the buoyancy-driven flow. The spatial variability of the surface heat flux is dominated by the cooling due to latent and sensible heat fluxes in winter [*Hirose et al.*, 1996]. This aspect is well represented by the simple parameterization of the heat flux used here. One could also superimpose a spatially uniform seasonal cycle to the heat flux in the marginal sea to represent the seasonal cycle in the radiative fluxes, but this would have little influence on the upper layer currents or annual mean exchange with the open ocean. The second point is that, during the summer months when there is large-scale heating, the eastern boundary current will begin to propagate toward the west at the baroclinic Rossby wave phase speed. For a phase speed of 1–2 cm s^{-1} and a summer heating season of April through August, the eastern boundary current would propagate only 150–300 km toward the west. The onset of cooling each winter would once again trap the eastern boundary current near the eastern boundary. *Kim and Yoon* (1996) find a similar offshore propagation of the Nearshore Branch during summer and fall in their wind- and buoyancy-forced primitive equation model of the JES.

[25] There will, in general, be cooling in the present model if the restoring thickness H^* is less than the maximum thickness of the wind-driven inflow, which for the present case $h_{max} = 0.05$. The circulation with even moderate cooling within the marginal sea is fundamentally different from that found with wind forcing only. The upper layer thickness for a case with $H^* = -0.2$, $\delta_T = 0.02$, and $\alpha = 15$ (strong damping east of the island) is shown in Figure 2b. The flow through the marginal sea remains anticyclonic, but the transport in the upper ocean is now split between an eastern boundary current and a western boundary current. The thickness in the interior of the basin is very nearly constant at h −0.18, and so the interior geostrophic flow is essentially zero. For these parameter settings, ~63% of the anticyclonic circulation through the marginal sea passes through the eastern boundary current, and the remaining 37% passes through the western boundary current. This splitting of the inflow into eastern and western boundary currents is qualitatively similar to the splitting of the Tsushima Current into the Second Branch and the East Korean Warm Current in the southern JES (Figure 1). (These parameters are not intended to simulate the actual conditions in the JES, but rather chosen to demonstrate the general influences of cooling in the marginal sea.) As will be shown in section 3, the wind-driven transport in the marginal sea would be carried primarily in the deeper layers, transmitted downward by the diapycnal mass flux out of the upper layer, and would thus enhance the western boundary current transport above that found here.

[26] A branching of the inflow transport into eastern and western boundary currents is generally found as long as $h_{min} < H^* < h_{max}$, where $h_{min} = -0.30$ is the minimum thickness of the water flowing into the marginal sea for wind forcing only. If the air-sea exchange is such that heating dominates and $H^* > h_{max}$, then nearly all of the inflow transport will be carried northward in the western boundary current. If the marginal sea is cooled sufficiently, so that $H^* < h_{min}$, the throughflow is carried in the eastern boundary current.

[27] The width of the eastern boundary current depends on the width of the thermal boundary layer δ_T. Figure 3a shows the

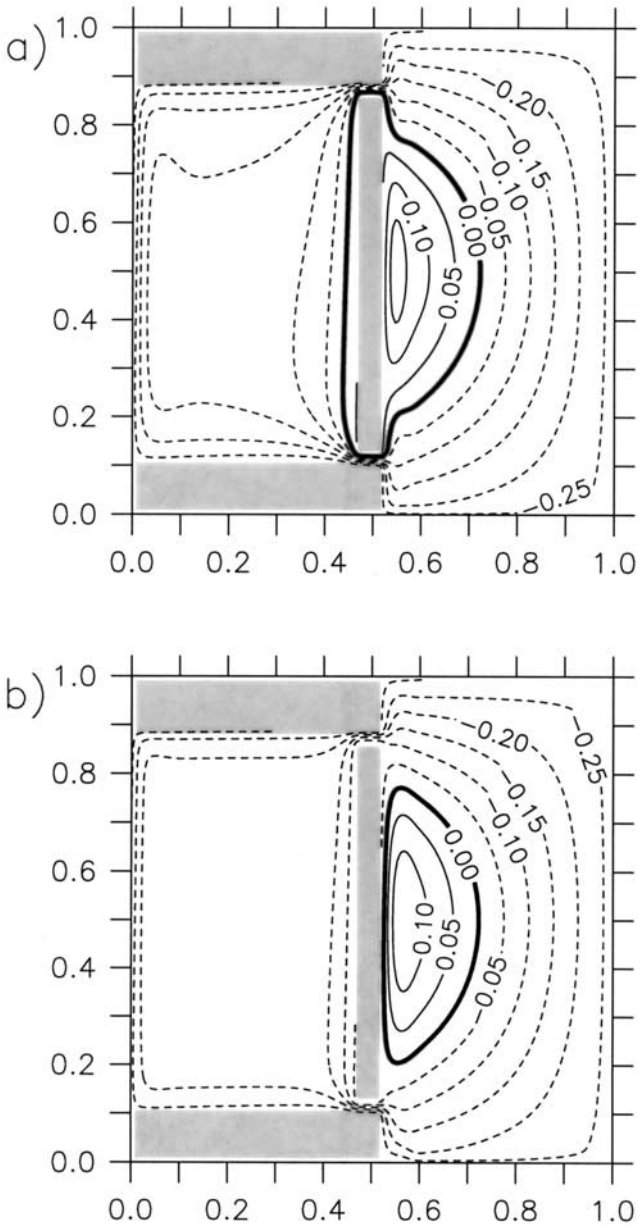

Figure 3. Upper layer thickness from a shallow water numerical model with wind and buoyancy forcing. (a) Strong damping to the east of the island (α = 15) and weak buoyancy forcing in the western basin δ_T = 0.06. (b) Weak damping to the east of the island (α = 0.2) and strong buoyancy forcing in the western basin δ_T = 0.02.

thickness for a case with δ_T = 0.06. A qualitatively similar branching of the inflow occurs, but now the eastern boundary current is wider and has a reduced transport compared to the case with δ_T = 0.02. The width increases because Rossby waves are able to propagate further toward the west before being damped by air-sea exchange. In the limit that $\delta_T = O(x_w)$, the eastern boundary current ceases to exist and the entire upper layer of the marginal sea is warmed to the maximum inflow temperature. This is the result found in numerical models that have an inflow of warm water but do not impose a cooling at the surface [e.g., *Yoon and Suginohara*, 1977]. The importance of the competition between westward propagation of Rossby waves and vertical mixing due to buoyancy forcing in maintaining the eastern boundary current was also noted in a realistic primitive equation model of the JES by *Hogan and Hurlburt* [2000]. The northward transport in the eastern boundary current decreases with increasing δ_T because the interior of the ocean is warmer than is found for smaller δ_T. This is consistent with the weaker air-sea exchange and the linear vorticity balance, as discussed in section 3.

[28] For the case of cyclonic wind stress curl and cooling, as is found for the Sea of Okhotsk, the inflow current does not branch into eastern and western boundary currents. This lack of branching is because the inflow is through the northern strait, and the less dense inflow waters flow so that the boundary is on the right in the Northern Hemisphere. The inflow current would bifurcate in a subpolar gyre situation only if there were warming in the marginal sea, a condition not found in the Sea of Okhotsk. This dependence on the sense of the large-scale wind stress curl and the surface heat flux in the marginal sea provides a simple explanation of why there is a branching of the inflow in the JES but not in the Sea of Okhotsk.

[29] The general character of the circulation in the marginal sea is not sensitive to the strength of damping along the eastern side of the island. The thickness on the island for a weak damping case (α = 0.2) has been reduced compared to the strong damping case (Figure 3b). The inflow now has a maximum value of h_{max} = −0.05, compared to h_{max}= 0.05 for the strong damping case. As a result, the stagnation points on the eastern side of the island are shifted toward the northern and southern tips of the island, and the recirculation region has expanded. Because v no longer changes sign on the eastern side of the island, it is clear that dissipation has become important along the western side of the island. The transport through the marginal sea is now slightly reduced, entirely at the expense of the transport in the eastern boundary current.

[30] The mechanisms by which the marginal sea adjusts to buoyancy forcing are highlighted by considering the difference between the upper layer thickness and the thickness to which the upper layer is being restored. The thickness anomaly $h - h^*$ for the strong damping case (α = 15) has a value in the interior of the marginal sea of 0.02 (Figure 4a). This is consistent with the linear vorticity balance and wind forcing, as discussed in section 3. The eastern boundary current and interior of the marginal sea have positive thickness anomalies and are thus cooled by the buoyancy-forcing term. The heat flux is proportional to the thickness anomaly so that the regions of strongest heat loss are found along the western side of the island. This is consistent with the annual mean heat flux in the JES calculated by *Hirose et al.* [1996]. Note that this buoyancy loss and downwelling will force a deep southward flowing countercurrent along the west coast of Japan, consistent with the observations and modeling study of *Kim and Yoon* [1999].

[31] For this choice of H^*, the western, northern, and southern boundary currents have negative anomalies and are heated. A more realistic cooling of these boundary currents would result if a spatially uniform heat loss were added to the spatially variable heat flux considered here, as is found in the data analysis of *Hirose et al.* [1996].

[32] The response in the eastern basin helps to understand how the exchange between the marginal sea and the open ocean adjusts to cooling. A band of negative anomalies extends through the southern strait and along the southern boundary into the open ocean. This anomaly is damped by the strong restoring before it can extend all the way around the open ocean perimeter. A similar anomaly extends from the northern strait along the eastern side of the island. For this case with large α, this anomaly is also damped before it can reach the southern tip of the island. It is important to note that the thickness anomaly is zero along the northern boundary of both straits. The negative thickness anomaly along the southern edge of the southern strait indicates that the inflow transport has increased compared to the wind-forced-only case. On the other hand, the outflow transport has decreased because the thickness on the northern tip of the island has decreased. The

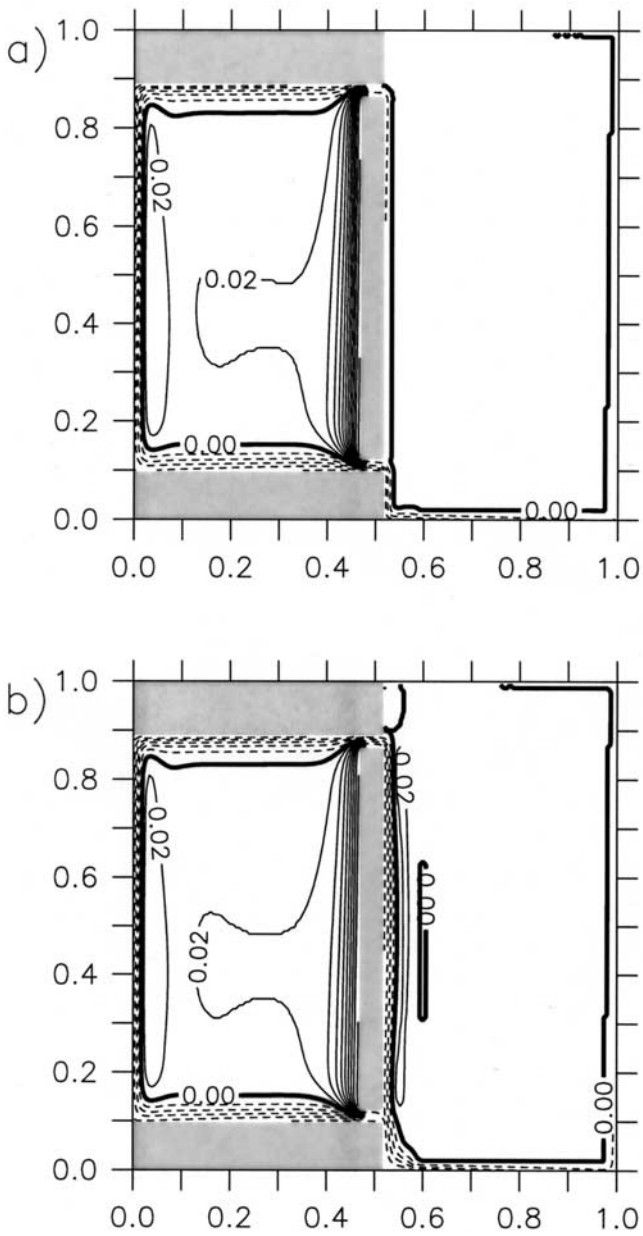

Figure 4. Difference in the upper layer thickness relative to the restoring layer thickness h^*. (a) Strong damping case $\alpha = 15$. (b) Weak damping case $\alpha = 0.2$.

difference in transport between the inflow and outflow is accounted for by downwelling in the marginal sea, as discussed further in the next section.

[33] The thickness anomaly for the small island case ($\alpha = 0.2$) is shown in Figure 4b. The thickness anomaly in the interior of the marginal sea is the same as that found for large α, but the values around the island are now very different. The ability of Kelvin waves to propagate freely along the eastern side of the island allows the thickness (or temperature) of the upper layer to be reduced in response to the cooling in the marginal sea. This effect is reflected by the lower value all along both the eastern and western sides of the island. By implication, the transport through both straits, and in the eastern boundary current, are less than for the strong damping case.

[34] Because Kelvin waves propagate with the coast to the right in the Northern Hemisphere, the minimum temperature of the water flowing out of the marginal sea through the northern strait is determined by the open ocean circulation, not the cooling in the marginal sea. On the other hand, the warmest water flowing into the open ocean is determined by the marginal sea circulation. Similarly, the coolest water flowing into the marginal sea from the open ocean is determined by the heat fluxes in the marginal sea, as indicated in Figure 4. The maximum temperature of the inflowing water is determined by either only the wind-driven open ocean circulation ($\alpha \gg 1$) or both cooling in the marginal sea and the large-scale wind forcing ($\alpha \ll 1$), depending on the dissipation of Kelvin waves on the eastern side of the island.

3. An Analytic Model of the Marginal Sea Circulation

[35] Understanding the structure of the currents in the marginal sea, and how the net transport through each of the straits depends on the model parameters and surface heat flux in the marginal sea, is aided by the development of a simple linear theory for the upper layer wind- and buoyancy-forced circulation. The starting point is the linear vorticity equation with lateral viscosity,

$$\beta^* v = f w_z + A_h \nabla^2 \zeta, \tag{2}$$

where $f = f_0 + \beta^* y$ is the Coriolis parameter, $w$is the vertical velocity, A_h is the lateral viscosity coefficient, $\zeta = v_x - u_y$ is the relative vorticity, v, u are the meridional and zonal velocities, and subscripts indicate partial differentiation. It will be assumed that the meridional velocity is in geostrophic balance and that the deep flow is motionless so that $v = p_x/f$ and, anticipating eastern and western boundary layers, $\partial u/\partial y \ll \partial v/\partial x$.

[36] The effects of a wind stress curl are imposed through the specification of w at the surface to be the Ekman pumping velocity.

$$w(z = 0) = w_e = curl(\tau/f) \tag{3}$$

The circulation may also be forced by restoring the upper layer thickness h towards a specified thickness H^* with timescale t_T. For simplicity, H^* is taken to be uniform over the marginal sea, although a meridional dependence is straightforward (Spall, submitted manuscript, 2001). Restoring the model thickness toward a specified thickness is a parameterization of buoyancy forcing by heat exchange with the atmosphere. When the upper layer is thicker than H^*, the layer thickness is reduced by transferring mass out of the upper layer and into the deep ocean. Because the lower layer is of higher density, this flux corresponds to cooling by the atmosphere and downwelling. This mass exchange with the deep ocean may be written in terms of the vertical velocity as

$$w(z = -h) = w_b = \frac{H^* - h}{t_T} = \frac{p^* - p}{t_T g'}, \tag{4}$$

where g' is the reduced gravity between the upper layer and the deep ocean and the integrated hydrostatic relations $p = g'h$ and $p^* = g'H^*$ have been used.

[37] The linear vorticity equation may now be written in terms of the pressure as

$$\beta^* p_x = \frac{f^2 w_e}{H} + \frac{f^2 (p - p^*)}{g' H t_T} + A_h p_{xxxx}, \tag{5}$$

where the mean thickness of the upper layer is $H$and it is assumed that the variations in the upper layer thickness are small compared to H (linearize the density equation). This approach is very idealized, but it does allow for relatively simple analytic solutions that make explicit the relationship between the general circulation

in the upper ocean of the marginal sea, the exchange rates, and the large-scale wind and buoyancy forcing.

[38] It is useful to nondimensionalize the vorticity equation with the following scaling.

$$p, p^* \propto V L f_0, \quad x, y \propto L, \quad v, u \propto V, \quad f = f_0(1 + \beta^* L y). \quad (6)$$

The nondimensional latitude y is now referenced to a central latitude y_0. Substitution into (5) results in a nondimensional equation for the pressure p.

$$p_{xxxx} - \left(\frac{L}{\delta_M}\right)^3 p_x + \left(\frac{L}{\delta_M}\right)^3 (1 + \beta y)^2 \left[w_e + \left(\frac{L}{\delta_T}\right)(p - p*)\right] = 0. \quad (7)$$

The boundary layer widths δ_M and δ_T are the same as in the previous section. It is useful to decompose the pressure field into a term that is independent of longitude, $\mathcal{P}(y)$, and an adjustment due to the presence of meridional boundaries $P(x, y)$. The pressure in the marginal sea interior, away from the lateral boundaries, is a function of latitude only,

$$\mathcal{P}(y) = p^* - w_e(y)\delta_T/L. \quad (8)$$

The upper layer pressure, or thickness, varies from the atmospheric value p^* by an amount proportional to the Ekman pumping rate and the nondimensional thermal boundary layer width. This is consistent with the thickness anomalies in the interior of the basin shown in Figures 2b and 3a.

[39] In the interior, using (4), the nondimensional vertical velocity at the base of the upper layer is simply

$$w_b = \frac{p^* - \mathcal{P}}{\delta_T/L} = w_e. \quad (9)$$

The Ekman pumping rate is exactly balanced by the diapycnal mass flux. The deep ocean would be put into motion by this diapycnal mass flux in the same way that in the absence of buoyancy forcing, the upper ocean would be forced by the wind. The balance between w_e and w_b indicates that there is no vertical shear in the meridional velocity away from the lateral boundaries.

[40] Zonal variability in the pressure arises as a result of the lateral boundaries. It is convenient in order to solve for the boundary layer structure to choose the lateral length scale as $L = \delta_M$, so that P satisfies

$$P_{xxxx} - P_x + (1 + \beta y)^2 \left(\frac{\delta_M}{\delta_T}\right) P = 0. \quad (10)$$

The solution to (10) is obtained by assuming the form

$$P(x, y) = A(y)e^{ikx}. \quad (11)$$

Substitution of (11) into (10) results in an equation for the roots k:

$$k^4 - ik + (1 + \beta y)^2 \left(\frac{\delta_M}{\delta_T}\right) = 0. \quad (12)$$

There are four roots to (12). The two roots with negative imaginary components, k_1 and k_2, provide bounded solutions extending from the eastern boundary. The two roots with positive imaginary components, k_3 and k_4, provide bounded solutions extending from the western boundary. The dependence of the roots on latitude y arises because the Rossby wave phase speed (which is represented in δ_T for the quasigeostrophic approximation) decreases as f^{-2} for planetary geostrophic dynamics.

[41] Although the general solution to (12) is quite complex, one can obtain useful approximate solutions for the roots in the limit of weak buoyancy forcing, $\delta_M/\delta_T \ll 1$. The thermal restoring timescale in the ocean can be estimated as $t_T = \rho_0 C_p H/Q$, where $\rho_0 = 1026$ kg m^{-3} is a reference density of seawater, $C_p \approx 4000$ J kg^{-1} °K^{-1} is the specific heat of seawater, $H \approx 100$ m is the thickness of the upper layer, and Q is the variation in surface heat flux arising from the air-sea temperature difference. *Hirose et al.* [1996] provide an estimate of Q to be 30 Wm^{-2} °K^{-1}. Using these values, $t_T = 1.3 \times 10^7$ s. Taking a typical midlatitude Rossby wave phase speed of 0.02 m s^{-1}, this gives a thermal boundary layer width of $O(250$ km). This is much larger than the typical Munk layer width of $O(50-100$ km), so that the limit $\delta_M/\delta_T \ll 1$ is appropriate for the JES. In this case, the eastern and western roots can be approximated from (12) as

$$k_1 = -1, \; k_2 = -i\delta_M/\delta_T, \; k_{3,4} = \left(i \pm \sqrt{3}\right)/2. \quad (13)$$

[42] The perturbation pressure $P$is now written as the sum of the eastern and western boundary layer solutions, each with an amplitude that varies in y.

$$P(x, y) = A(y)e^{ik_1(x - x_w)} + B(y)e^{ik_2(x - x_w)} + C(y)e^{ik_3 x} + D(y)e^{ik_4 x}. \quad (14)$$

The relationships between the coefficients $A(y)$ and $B(y)$, and $C(y)$ and $D(y)$, are provided by the lateral boundary condition on the meridional velocity. For no-slip boundaries, $v = P_x = 0$ at $x = 0$ and $x = x_w$ so that

$$B(y) = -\frac{k_1}{k_2}A(y), \; D(y) = -\frac{k_3}{k_4}C(y). \quad (15)$$

[43] The meridional momentum equation and the no-normal flow boundary condition at $x = x_w$ are used to solve for the meridional dependence of the perturbation pressure $A(y)$. The nondimensional form of the steady, linear meridional momentum equation may be written in terms of the perturbation pressure as

$$(1 + \beta y)u + P_y = \frac{\beta P_{xxx}}{(1 + \beta y)}. \quad (16)$$

At the eastern boundary, the no-normal flow condition requires that $u = 0$, so that

$$(1 + \beta y)P_y = \beta P_{xxx}. \quad (17)$$

Substitution of (14) at $x = x_w$, with (15), into (17) results in a single equation for the function $A(y)$

$$(1 + \beta y)A_y = C_1 A, \quad (18)$$

where the constant $C_1 = i\beta k_1 k_2(k_1 + k_2)$. Making use of the approximate values for the roots k_1 and k_2 (13) for $\delta_M/\delta_T \ll 1$, $C_1 = -\beta\delta_M/\delta_T$.

[44] The general closed form solution for $A(y)$, with the boundary condition that $h = h_i$ at $x = x_w$, is

$$A(y) = \frac{h_i k_2}{k_2 - k_1}(1 + \beta y)^{C_1/\beta}. \quad (19)$$

In the limit $\delta_M/\delta_T \ll 1$ and making use of (13), a useful approximate solution is

$$A(y) = \frac{h_i k_2}{k_2 - k_1}(1 - \delta_M/\delta_T \beta y). \tag{20}$$

[45] A similar procedure yields the thickness on the western boundary, in the limit that $\delta_M/\delta_T \ll 1$, to be

$$C(y) = \frac{h_0 k_4}{k_4 - k_3}(1 - \beta y). \tag{21}$$

To first order in β, the amplitude of the pressure is constant on the island and along the western boundary. For weak buoyancy forcing ($\delta_M/\delta_T \ll 1$), the change in layer thickness with latitude in the eastern boundary current at $x = x_w$ is much less than the change in layer thickness in the western boundary current at $x = 0$.

[46] The upper layer thickness may now be written as the sum of the interior thickness h_{int} and the adjustments due to the lateral boundaries as

$$h(x,y) = h_{\text{int}} + \frac{(h_i - h_{\text{int}})}{k_2 - k_1}\left[k_2 e^{ik_1(x-x_w)} - k_1 e^{ek_2(x-x_w)}\right](1 - \delta_M/\delta_T \beta y) + \frac{(h_0 - h_{\text{int}})}{k_4 - k_3}\left[k_4 e^{ik_3 x} - k_3 e^{ik_4 x}\right](1 - \beta y), \tag{22}$$

where the nondimensional hydrostatic relation $h = P$ has been used. Following (8), the thickness of the upper layer in the interior of the basin, h_{int}, differs from that to which it is restored H^* by an amount required to balance the wind stress curl

$$h_{\text{int}} = H^* + \frac{\delta_T}{L}\tau_y(1 + \beta y). \tag{23}$$

[47] The transport in the eastern boundary current depends on the difference between the temperature on the island, h_i, and the temperature in the marginal sea interior, h_{int}. If the island is warmer than the basin interior (as required for cooling in the marginal sea) then an eastern boundary current with northward transport will result.

[48] The thickness on the western boundary at the northern strait, h_0, is set by the open ocean circulation via Kelvin wave propagation. Because the open ocean is strongly restored to the wind-forced-only thickness, the value of h_0 can be taken directly from the reference calculation. It seems reasonable to assume that, if the open ocean basin is sufficiently large, Kelvin waves would be entirely damped before they can propagate all the way around the open ocean basin.

[49] The direction of the transport in the western boundary current (relative to the deep circulation) is controlled by the sign of $h_0 - h_{\text{int}}$. If the atmosphere is sufficiently warm that $h_0 - h_{\text{int}} < 0$, then the transport in the western boundary current is northward. If cooling is sufficiently strong to reverse the pressure gradient near the western boundary, then the transport in the western boundary current (relative to the deep flow) is to the south. In this case, the transport in the eastern boundary current is larger than the inflow transport, with the excess recirculating cyclonically in the marginal sea. However, the present solutions do not include the wind-driven western boundary current, which may be stronger than the buoyancy-driven western boundary current considered here.

[50] The value of h on the island can be determined by integrating the momentum equation tangent to a path that encircles the island. Following the approach of *Godfrey* [1989], a circulation path is chosen that extends from the eastern boundary of the open ocean around the western side of the island (Figure 5). The southward transport in the open ocean at $y = y_n$ is T_n and the southward transport at $y = y_s$ is T_s. Because buoyancy forcing is allowed, the meridional transport in the open ocean at the northern and southern latitudes of the island need not be the same. The transport at the southern latitude is related to the transport at the northern latitude by $T_s = T_n + W$, where W is the total amount of upwelled water to the east of the island. It is useful to write the transport at the northern latitude as the sum of the purely wind-driven transport T and a perturbation due to cooling in the marginal sea, T'. The circulation integral may then be written as

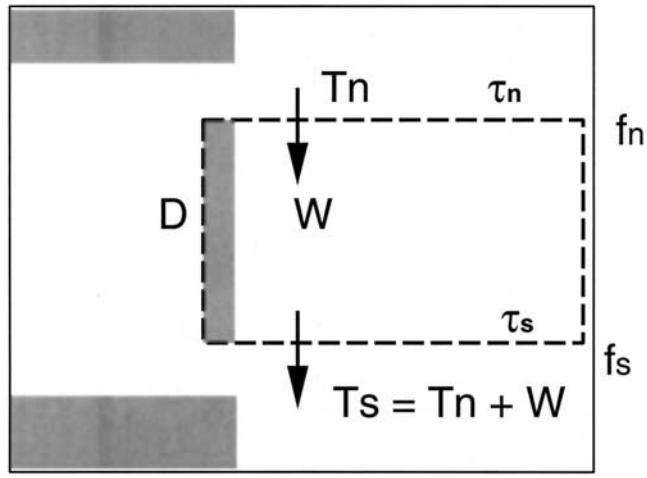

Figure 5. Schematic of the circulation around an island with upwelling to the east of the island W. The circulation integral is provided by integrating the momentum equations tangent to the dashed contour. Dissipation along the western side of the island is indicated by D.

$$(T + T')f_n - (T + T')f_s - Wf_s = \beta\Delta\tau(1 - x_e) + D, \tag{24}$$

where $\Delta\tau$ is the change in wind stress between y_s and y_n and D represents the dissipation along the western side of the island. The wind-driven transport T is the same as results from the standard island rule of *Godfrey* [1989], $T = \Delta\tau(1 - x_e)/(y_n - y_s)$. The change in transport due to buoyancy-forcing in the marginal sea, T', may then be written as

$$T' = \frac{Wf_s}{\beta L_i} + \frac{D}{\beta L_i}. \tag{25}$$

The circulation around the island is altered from the purely wind-driven case by either upwelling to the east of the island W or dissipation along the western side of the island D. These cases were considered for an imposed upwelling distribution by *Spall* [2000]. For the present problem the upwelling W and the dissipation D depend on the ocean circulation and the model parameters.

[51] The dissipation is calculated from the boundary layer solution for h (22) as

$$D = \int_{y_s}^{y_n} A_h v_{xx}(x = x_w)\, dy = -i\beta L_i k_1 k_2 (k_1 + k_2)(h_i - h_{\text{int}}). \tag{26}$$

In the weak buoyancy-forcing limit, $\delta_M/\delta_T \ll 1$ and the approximate roots $k_1$and k_2 (13) yield a simple estimate of the dissipation along the western boundary of the island.

$$D = -\beta L_i \delta_M/\delta_T \left(\bar{h}_i + h' - h_{\text{int}}\right). \tag{27}$$

The thickness on the island has been written as the sum of the purely wind-driven value $\bar{h}_i$ and the change due to buoyancy forcing h'. The dissipation increases linearly with the meridional extent of the island L_i, with β, and with the relative strength of thermal forcing (δ_M/δ_T). The dissipation also increases with the difference between the thickness on the island and the thickness in the marginal sea interior.

[52] The upwelling to the east of the island W depends on the strength of the thermal restoring term to the east of the island. If $\alpha \ll 1$, Kelvin waves propagate the full length of the island without significant modification so that in this limit, $W = 0$. Substituting (27) into (25) with $W = 0$ and $h'_i = f_n T'$ gives the thickness anomaly at the northern tip of the island to be

$$h' = \frac{f_n \delta_M/\delta_T (\bar{h}_i - h_{\text{int}})}{1 + f_n \delta_M/\delta_T}. \tag{28}$$

[53] If $\alpha \gg 1$, Kelvin waves are damped before they can reach the southern limit of the island. The upwelling required to bring the meridional transport back to the purely wind-driven value at $y = y_s$ is $W = -T'$. Combining this with (27) and (25) gives the thickness anomaly at the northern tip of the island to be

$$h' = \frac{\beta L_i \delta_M/\delta_T (\bar{h}_i - h_{\text{int}})}{1 + \beta L_i \delta_M/\delta_T}. \tag{29}$$

[54] In both cases, the change in thickness at the northern tip of the island is negative for cooling in the marginal sea, indicating a reduction in outflow transport. The amplitude increases with the difference in wind-driven temperature on the island compared to that in the interior, and also with decreasing thermal boundary layer width δ_T. The terms in the numerator are a result of dissipation in the eastern boundary current for a transport equal to the wind-forced-only case. The actual dissipation is reduced relative to the wind-forced only case as the temperature on the island is decreased, giving rise to the terms in the denominator proportional to δ_M/δ_T.

[55] In general, for $\beta L_i \ll f_n$, the thickness anomaly at the northern tip of the island is smaller for the case of a large island than it is for the case of a small island. This result implies that the transport through the northern and southern straits will be more sensitive to heat fluxes in the marginal sea when Kelvin waves can propagate all the way around the island.

[56] The thickness anomaly $h - h^*$ at the midlatitude of the marginal sea found in the numerical model from the calculations in Figure 4 are compared to the theory (22), using (28) or (29) in Figure 6. The theory compares closely with the numerical results at all longitudes and for both the large and small island cases. The meridional flow is clearly divided into eastern and western boundary currents whose transports largely depend on the temperature on the western boundary, the temperature on the island, and the atmospheric temperature in the interior. The layer thicknesses in the interior and western boundary regions are independent of the damping to the east of the island. The layer thickness on the island is smaller for the case of weak damping in the eastern basin because the cooling effect is permitted to communicate around the island.

[57] It is clear from these results that the branching of the throughflow into eastern and western boundary currents in this model is simply a result of the atmosphere controlling the temperature of the upper ocean in the interior of the basin, and the wind forcing in the open ocean largely controlling the temperature on the western boundary and on the island. Geostrophy requires an eastern boundary current when the interior of the marginal sea is cooled. A subpolar gyre subject to strong cooling would not experience a branching of the inflow current into eastern and western boundary currents because the inflow would be through the northern strait and all of the flow would turn to the right.

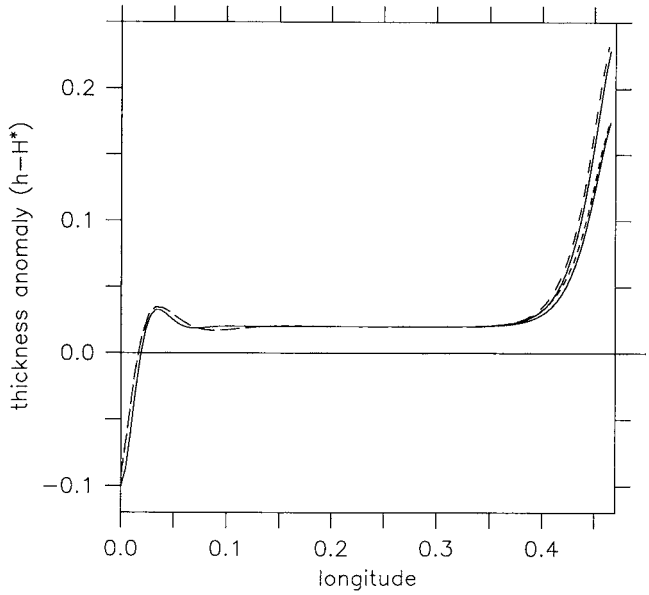

Figure 6. Comparison between the shallow water numerical model and theory for the upper layer thickness anomaly at the midlatitude of the basin. Solid lines, numerical model. Dashed lines, theory. The weak damping cases have the lower value of $h - H^*$ on the island.

[58] There also exist boundary layers along the northern and southern boundaries of the marginal sea. Although an exact analytic solution of these boundary layers is very difficult to obtain, particularly when buoyancy forcing is active, a simple scale analysis provides some useful insights into the balances and length scales of the flow. The appropriate nondimensional vorticity equation is

$$P_{yyyy} - \left(\frac{l}{\delta_M}\right)^3 \left(\frac{l}{L}\right) P_x - \left(\frac{1}{\delta_M}\right)^3 \left(\frac{1}{\delta_T}\right) P = 0, \tag{30}$$

where l is the meridional length scale of the boundary current. Near the straits in the marginal sea, where variations in x are important, the dominant balance is between the first and second terms. This balance yields is the familiar adiabatic northern and southern boundary layers that grow slowly to the west as $l \propto \delta_M^{3/4} x^{1/4}$. However, for distances greater than $O(\delta_T)$ from the inflow or outflow straits, the boundary layer width becomes independent of x and the dominant balance is between the first and third terms (see Figures 3a and 3b). Vertical motions induced by the buoyancy forcing are balanced by viscous fluxes into the boundary. The width of this boundary layer scales as $l = (\delta_T/\delta_M)^{1/4} \delta_M$. For even very weak buoyancy forcing, the meridional length scale of the northern and southern boundary layers is close to the Munk layer width.

[59] This simple analytic model provides an estimate of the upper layer thickness in the marginal sea given: wind stress curl, viscous boundary layer width δ_M, thermal boundary layer width δ_T, the atmospheric temperature H^* in the marginal sea; and the strengthof the thermal forcing on the eastern side of the island. From the layer thickness, one can calculate the horizontal circulation, exchange rates, and the regions of water mass conversion and downwelling within the marginal sea.

4. Exchange and Downwelling

[60] The dependence of the exchange with the open ocean and downwelling within the marginal sea on the model parameters is now investigated. The main issue of interest is how heat fluxes in

the marginal sea influence the transport into the marginal sea, the downwelling, and the transport out of the marginal sea. The simple analytic model provides direct estimates of these quantities and their parameter dependence, and the shallow water numerical model provides a useful benchmark to test the theory.

[61] The key unknown in the problem is the layer thickness on the island, h'. The thickness in the interior is controlled by the atmospheric temperature H^*, the wind stress curl, and the relative strength of air-sea exchange through δ_T (23). The thickness on the western boundary is essentially determined by the minimum outflow thickness, which is controlled by the wind-forced open ocean circulation. (There is only a weak dependence of h on the basin perimeter with latitude, as specified through $C(y)$.) The thickness on the island is determined by the circulation integral and is influenced by the strength of dissipation along the western side of the island and the amount of upwelling in the open ocean (25). Once the island thickness, or temperature, is known, the solution is given by (22).

[62] A series of numerical model calculations have been carried out in which the restoring thickness H^* and the relative thermal forcing strength δ_T/δ_M are varied. Decreasing H^* represents a colder atmosphere over the marginal sea. For values of $H^* < 0.05$ there is cooling in the marginal sea, while for values of $H^* < -0.30$ the atmospheric temperature is less than the coolest inflow waters for the wind-driven-only problem. Increasing δ_T/δ_M represents a decrease in the surface heat flux for a given air-sea temperature difference.

[63] The change in thickness at the northern tip of the island resulting from a net heat flux in the marginal sea is shown in Figure 7a for weak Kelvin wave damping ($\alpha = 0.2$). The thickness anomaly at the northern tip of the island increases nearly linearly with δ_T/δ_M and with H^*, as expected from (28). There is very little change from the wind-driven solution when the atmospheric temperature is close to the warmest inflow waters. However, once H^* drops below this inflow thickness, cooling ensues and an eastern boundary current is formed. Once the eastern boundary current exists, dissipation along the western coast of the island becomes important and the net circulation around the island is altered. As shown by the circulation integral (25), the flow through the northern strait, and hence the thickness of the upper layer, must decrease when downwelling is located near the western coast of the island. This change in transport is balanced by a cooling of the waters all around the island.

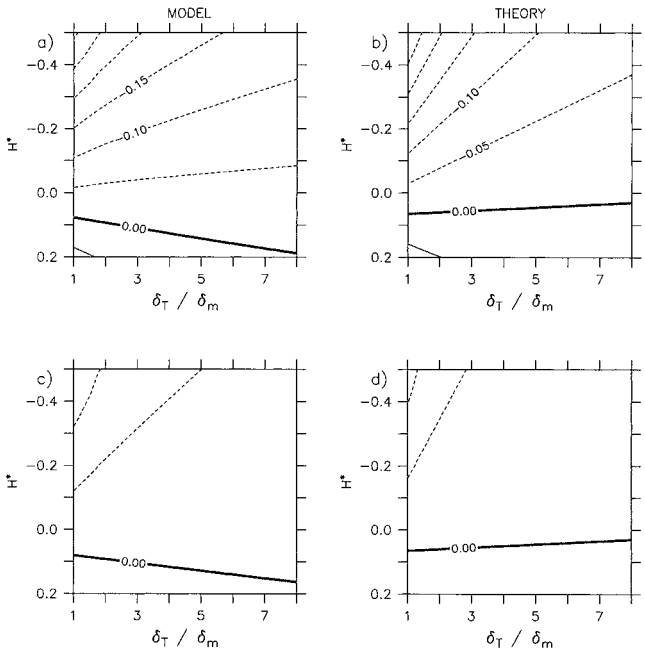

Figure 7. Change in upper layer thickness at the northern tip of the island due to buoyancy forcing in the marginal sea as a function of atmospheric temperature H^* and restoring strength δ_T/δ_M. (a) Shallow water model with weak damping $\alpha = 0.2$. (b) Theory with weak damping $\alpha = 0.2$. (c) Shallow water model with strong damping $\alpha = 15$. (d) Theory with strong damping $\alpha = 15$.

[64] The change in layer thickness at the northern tip of the island predicted by the theory (28) is examined for the same range of model parameters (Figure 7b). The theory generally agrees well with the numerical model results. There are some small differences, but the general dependence on atmospheric temperature and thermal boundary layer width is well represented by the theory. One would not expect an exact comparison because the theory neglects corner effects and makes the weak buoyancy-forcing approximation in estimating the dissipation along the western side of the island.

[65] The layer thickness changes for strong damping ($\alpha = 15$) in the numerical model and that predicted by the theory (29) are examined (Figures 7c and 7d). Again, the agreement between theory and model is generally good. The most important result is that the layer thickness at the northern tip of the island is much less sensitive to variations in heat flux within the marginal sea when Kelvin waves are not permitted to propagate around the island. Although dissipation remains strong along the western coast of the island, the decrease in circulation around the island is largely offset by an increase required to balance the net upwelling to the east of the island as the Kelvin waves are damped. Upwelling to the east of an island requires a circulation around the island to balance both mass and potential vorticity budgets, as discussed by *Spall* [2000].

[66] The change in transport from the marginal sea into the open ocean through the northern strait is proportional to h'. The outflow transport is relatively insensitive to heat flux in the marginal sea for the large island but decreases substantially with increasing cooling for the small island. The transport is most sensitive to heat flux over the marginal sea for small δ_T. This is because the dissipation increases as δ_T decreases and the eastern boundary current becomes narrow.

[67] Using the continuity equation (A2), the total amount of water downwelled within the marginal sea is calculated by integrating over the marginal sea

$$W = \int_{y_o}^{y_0+L_y} \int_0^{x_w} (h - H^*)(\beta/\delta_T)\, dx\, dy. \tag{31}$$

If the marginal sea is wide, so that $\delta_T/L_x \ll 1$, this integral may be approximated as

$$W = \beta L_i \left[\tau_y x_w - i(h_i - h_{\text{int}}) \frac{(k_1 + k_2)}{k_1 k_2} \frac{\delta_M}{\delta_T} + i(h_0 - h_{\text{int}}) \frac{(k_3 + k_4)}{k_3 k_4} \frac{\delta_M}{\delta_T} \right] + 2\beta x_w (\delta_T/\delta_M)^{1/4} \delta_M (h_0 - h_{\text{int}}). \tag{32}$$

There are four contributions to the vertical motion. The first term on the right-hand side is the Ekman pumping rate. The thickness anomaly in the basin interior is determined so that the diapycnal mixing rate exactly balances the Ekman pumping rate, there is no stretching in the vertical, and the geostrophic meridional velocity is zero. The second contribution comes from downwelling in the eastern boundary current. For cooling, this current is anomalously warm compared to h_{int} so that the thermal forcing term drives a cooling and downwelling near the eastern boundary. The third term

reflects the influence of buoyancy exchange in the western boundary current. For moderate cooling, the western boundary region is cooler than the interior and is a region of upwelling and warming. The final term is the approximate upwelling in the northern and southern boundary layers, taking the boundary layer width from scaling (30). For moderate cooling, this term will generally result in upwelling, as found in the western boundary layer.

[68] The relative contributions of the boundary layer regions are made clearer by considering the limit of weak buoyancy forcing, $\delta_M/\delta_T \ll 1$. Substitution of the approximate roots (13) into (32) gives

$$W = \beta L_i \left[\tau_y x_w + h_i - h_{\text{int}} + (h_0 - h_{\text{int}}) \frac{\delta_M}{\delta_T} \right] + 2\beta x_w \delta_M (h_0 - h_{\text{int}}). \tag{33}$$

For $\delta_M \ll \delta_T, L_i$, the vertical motions are dominated by the Ekman pumping in the interior and the cooling in the eastern boundary current. The upwelling in the western boundary current is generally small when buoyancy forcing is relatively weak. The downwelling increases with β, L_i, the island temperature h_i, the wind stress curl τ_y, the basin width x_w, and decreasing H^* (recall that $h_{\text{int}} = H^* + \delta_T \tau_y (1 + \beta y)$).

[69] The downwelling within the marginal sea has been calculated from a series of numerical model calculations as a function of the thermal damping strength δ_T and the atmospheric temperature H^* (Figure 8a) for $\alpha = 15$. For weak thermal forcing ($\delta_T/\delta_M \gg 1$), the downwelling increases linearly with H^*, as expected from (33). The downwelling increases slightly with decreasing δ_T for strong cooling. This dependence on δ_T reflects the change in the roots $k_{1,2}$ for the eastern boundary layer, not represented in the weak forcing limit (33). The theoretical estimate for the downwelling in the marginal sea (32) with (29) is shown in Figure 8b. The theory compares well with the numerical results. For weak cooling, the downwelling is dominated by the Ekman pumping term, while for strong cooling, the downwelling is dominated by the buoyancy loss in the eastern boundary current.

[70] The theory also compares well with the numerical model results for the small island cases with $\alpha = 0.2$ (not shown). The overall pattern is the same as the large island case but the downwelling is slightly weaker. This is because the pressure on the island is reduced when Kelvin waves are permitted to transmit the influences of cooling in the marginal sea all the way around the island. The lower pressure on the island reduces the transport in the eastern boundary current and, as a result, the subsequent downwelling. The downwelling in the interior is insensitive to the thermal forcing east of the island because it is controlled by the wind stress curl.

[71] The inflow into the marginal sea is determined by the sum of the outflow through the northern strait and the downwelling within the marginal sea. Because the outflow transport does not vary strongly for the large island case, the downwelling must be supplied largely by increasing the inflow transport over the wind-only case. The maximum thickness of the inflow is fixed at the wind-driven value, so that this transport must be balanced by a decrease in the minimum thickness (or temperature) of the inflowing water. This result is an example of the processes in the marginal sea controlling the conditions of the inflow upstream of the marginal sea. As a consequence, the inflow varies strongly with the restoring thickness H^* for the large island. The inflow is less sensitive to H^* for a small island because the outflow transport decreases with decreasing H^* so that the net circulation through the marginal sea is also reduced.

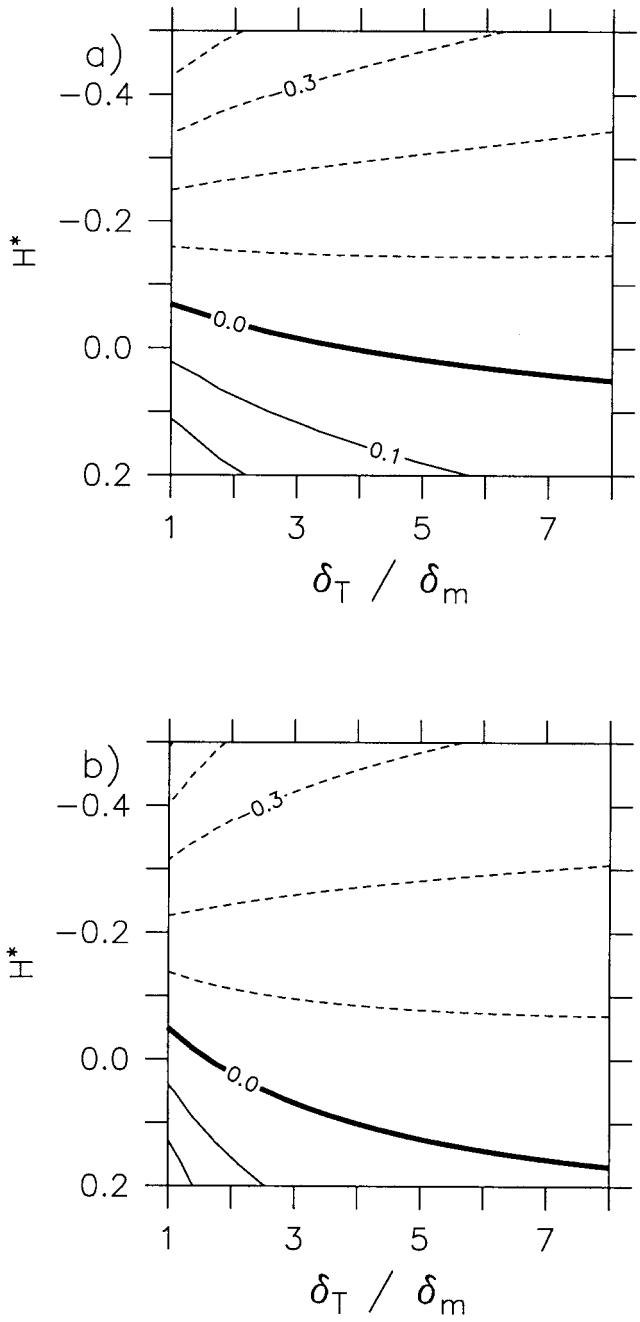

Figure 8. Total downwelling with the marginal sea for strong damping ($\alpha = 15$) as a function of atmospheric temperature H^* and restoring strength δ_T/δ_M. (a) Diagnosed from the shallow water numerical model. (b) Theory.

5. Summary

[72] The wind- and buoyancy-forced upper ocean circulation in a marginal sea that is connected to the open ocean by more than one strait has been explored using simple numerical and analytical models. The inflow transport was found to branch into eastern and western boundary currents when the large-scale wind stress curl is anticyclonic and there is cooling in the marginal sea. The basic reason for this branching is that the temperature in the interior of the marginal sea is controlled by the atmospheric temperature while the temperature on the island is largely controlled by the wind forcing in the open ocean. For anticyclonic wind stress curl in the open ocean, the warm water flows into the marginal sea with the island on the right (Northern Hemisphere). Atmospheric cooling traps this warm water near the eastern boundary. Geostrophy then requires an upper ocean eastern boundary current.

[73] Linear theory is used to calculate the wind- and buoyancy-forced upper layer thickness (or temperature) in the marginal sea as

a function of the temperature on the island, the temperature on the basin perimeter, and the atmospheric temperature. A circulation integral around the island provides the necessary constraint to solve for the temperature on the island, which is the primary unknown in the problem. The boundary layer solution then gives the upper ocean layer thickness, horizontal transports, and regions of water mass transformation as a function of atmospheric temperature, wind forcing, and viscous and thermal boundary layer widths. The thickness on the island, and hence the inflow and outflow transports and downwelling within the marginal sea, depends on whether or not Kelvin waves are able to propagate all the way around the island before being dissipated. Solutions for weak and strong damping of Kelvin waves are provided and compare closely with numerical model results. These results indicate that the properties of the inflow and outflow depend on the processes within both the marginal sea and the open ocean.

[74] The branching of the inflow current into eastern and western boundary currents is qualitatively similar to the observed splitting of the Tsushima Current in the southern Japan/East Sea. A similar branching is not found for marginal seas subject to cooling and cyclonic wind stress curl, such as is the Sea of Okhotsk. These results suggest that buoyancy forcing in the JES may play an important role in the formation and maintainence of the eastern branch of the Tsushima Current.

Appendix A: Shallow Water Numerical Model

[75] The nondimensional shallow water momentum equations may be written as

$$R(\mathbf{v}_t + \mathbf{v}\cdot\nabla\mathbf{v}) + (1+\beta y)\mathbf{k}\times\mathbf{v} = -\nabla h + E\nabla^2\mathbf{v}$$
$$+\beta\left(\tau/H\left(1+RB^{-1}h\right)\right), \qquad \text{(A1)}$$

where $\mathbf{v}$ is the horizontal velocity vector, h is the layer thickness, and τ is the wind stress. The continuity equation is written as

$$h_t + BR^{-1}\nabla\cdot\mathbf{v} + \nabla\cdot(\mathbf{v}h) = \gamma(h-h^*). \qquad \text{(A2)}$$

The variables have been nondimensionalized by a velocity scale U, a horizontal length scale L, and a vertical length scale H. The deviation of the layer thickness h from the motionless value is scaled as f_0UL/g'. The Coriois parameter is assumed to vary linearly with latitude as $f = f_0 + \beta^* y$, where f_0 is the Coriolis parameter at the central latitude of the domain and β^* is the dimensional variation of the Coriolis parameter with latitude. The reduced gravity between the moving layer and the deep ocean is g'. Time has been nondimensionalized with the advective timescale L/U, and the wind stress is nondimensionalized by $\rho_0 U\beta^* L$. This scaling results in several nondimensional numbers. The Rossby number $R = U/fL$ is a measure of the strength of the nonlinear terms. The Ekman number $E = A_h/f_0L^2$, where A_h is a Laplacian viscosity coefficient, measures the strength of dissipation. The variation of the Coriolis parameter over the meridional scale of the domain is measured by $\beta = \beta^* L/f_0$. The Burger number $B = (L_d/L)^2$, where $L_d = \sqrt{g'h}/f_0$ is the internal deformation radius.

[76] The model may also be forced by restoring of the layer thickness toward a specified thickness h^*, the last term on the right-hand side of (A2). If the upper layer is thicker than h^*, then the restoring acts to remove mass from the upper layer into the deep ocean. Since the deep ocean is cooler than the upper layer, this represents an increase in density and thus cooling in this simple model. Similarly, increasing the upper layer thickness via the restoring term represents heating. The strength of this buoyancy forcing is measured by $\gamma = L/Ut_T$, which is the ratio of the advective timescale to t_T, the timescale at which the interface is restored toward h^*.

[77] The model is integrated on a staggered C grid, and the equations are solved using a second-order centered finite difference scheme. Time stepping is achieved with a third-order accurate Adams-Bashforth scheme. The lateral boundary conditions are no-slip and no-normal flow.

[78] **Acknowledgments.** Support for this work was provided by the National Science Foundation under grant OCE-9818337 and by the Office of Naval Research under grant N00014-01-1-0165. Karl Helfrich provided helpful comments on an earlier version of this manuscript. This is Woods Hole Oceanographic Institution contribution 10449.

References

Cho, Y.-K., and K. Kim, Branching mechanism of the Tsushima Current in the Korea Strait, *J. Phys. Oceanogr.*, *30*, 2788–2797, 2000.

Godfrey, J. S., A Sverdrup model of the depth-integrated flow for the World Ocean, allowing for island circulations, *Geophys. Astrophys. Fluid Dyn.*, *45*, 89–112, 1989.

Hase, H., J.-H. Yoon, and W. Koterayama, The current structure of the Tsushima Warm Current along the Japanese coast, *J. Oceanogr.*, *55*, 217–235, 1999.

Hirose, N., C.-H. Kim, and J.-H. Yoon, Heat budget in the Japan Sea, *J. Oceanogr.*, *52*, 553–574, 1996.

Hogan, P. J., and H. E. Hurlburt, Impact of upper ocean-topographical coupling and isopycnal outcropping in Japan/East Sea models with 1/8 degree to 1/64 degree resolution, *J. Phys. Oceanogr.*, *30*, 2535–2561, 2000.

Kawabe, M., Branching of the Tsushima Current in the Japan Sea, part I, Data analysis, *J. Oceanogr. Soc. Jpn.*, *55*, 185–195, 1982a.

Kawabe, M., Branching of the Tsushima Current in the Japan Sea, part II, Numerical experiment, *J. Oceanogr. Soc. Jpn.*, *38*, 183–192, 1982b.

Kim, C.-H., and J.-H. Yoon, A numerical modeling of the upper and intermediate layer circulation in the East Sea, *J. Oceanogr.*, *55*, 327–345, 1999.

Minato, S., and R. Kimura, Volume transport of the western boundary current penetrating into a marginal sea, *J. Oceanogr. Soc. Jpn.*, *36*, 185–195, 1980.

Na, J.-Y., J.-W. Seo, and S.-K. Han, Monthly-mean sea surface winds over the adjacent seas of the Korea Peninsula, *J. Oceanogr. Soc. Korea*, *27*, 1–10, 1992.

Nof, D., The penetration of Kuroshio water into the Sea of Japan, *J. Phys. Oceanogr.*, *23*, 797–807, 1993.

Nof, D., Why much of the Atlantic circulation enters the Carribean Sea and very little of the Pacific circulation enters the Sea of Japan, *Prog. Oceanogr.*, *45*, 39–67, 2000.

Ou, H.-W., A model of buoyant throughflow: With application to branching of the Tsushima Current, *J. Phys. Oceanogr.*, *31*, 115–126, 2001.

Pedlosky, J., L. J. Pratt, M. A. Spall, and K. R. Helfrich, Circulation around islands and ridges, *J. Mar. Res.*, *55*, 1199–1251, 1997.

Preller, R. H., and P. J. Hogan, Oceanography of the Sea of Okhotsk and the Japan/East Sea, in *The Sea*, vol. 11, *The Global Coastal Ocean: Regional Studies and Syntheses*, edited by A. R. Robinson and K. H. Brink, 429–481, John Wiley, New York, 1998.

Sekine, Y., Wnd-driven circulation in the Japan Sea and its influence on the branching of the Tsushima Current, *Prog. Oceanogr.*, *17*, 297–312, 1986.

Spall, M. A., Buoyancy-forced circulations around islands and ridges, *J. Mar. Res.*, *58*, 957–982, 2000.

Wajsowicz, R. C., The circulation of the depth-integrated flow around an island with application to the Indonesian throughflow, *J. Phys. Oceanogr.*, *23*, 1470–1484, 1993.

Yoon, J.-H., Numerical experiment on the circulation in the Japan Sea, part III, Mechanism of the Nearshore Branch of the Tsushima Current, *J. Oceanogr. Soc. Jpn.*, *38*, 125–130, 1982a.

Yoon, J.-H., Branching of the Tsushima Current in the Japan Sea, part II, Numerical experiment, *J. Oceanogr. Soc. Jpn.*, *38*, 183–192, 1982b.

Yoon, J.-H., and N. Suginohara, Behavior of warm water flowing into a cold ocean, *J. Oceanogr. Soc. Jpn.*, *33*, 272–282, 1977.

M. A. Spall, Department of Physical Oceanography, Woods Hole Oceanographic Institution, Mail Stop 21, Clark 311A, 360 Woods Hole Road, Woods Hole, MA, 02543, USA. (mspall@whoi.edu)